General Disclaimer

One or more of the Following Statements may affect this Document

- This document has been reproduced from the best copy furnished by the organizational source. It is being released in the interest of making available as much information as possible.

- This document may contain data, which exceeds the sheet parameters. It was furnished in this condition by the organizational source and is the best copy available.

- This document may contain tone-on-tone or color graphs, charts and/or pictures, which have been reproduced in black and white.

- This document is paginated as submitted by the original source.

- Portions of this document are not fully legible due to the historical nature of some of the material. However, it is the best reproduction available from the original submission.

NATIONAL AERONAUTICS AND SPACE ADMINISTRATION

Technical Memorandum 33-387

Scaling of a High-Performance Ion Thruster

Eugene V. Pawlik

JET PROPULSION LABORATORY
CALIFORNIA INSTITUTE OF TECHNOLOGY
PASADENA, CALIFORNIA

July 15, 1968

NATIONAL AERONAUTICS AND SPACE ADMINISTRATION

Technical Memorandum 33-387

Scaling of a High-Performance Ion Thruster

Eugene V. Pawlik

Approved by:

D. R. Bartz, *Manager*
Research and Advanced Concepts Section

JET PROPULSION LABORATORY
CALIFORNIA INSTITUTE OF TECHNOLOGY
PASADENA, CALIFORNIA

July 15, 1968

Contents

I. Introduction 1

II. Thruster Scaling 1

III. Thruster Operation 5

IV. Conclusions 7

References 8

Table

1. Typical thruster performance data for a 10-magnet configuration 6

Figures

1. SERT II and scaled 20-cm-diam thrusters compared, cross-sectional sketch . . . 1

2. The 20-cm-diam permanent magnet electron-bombardment ion thruster 2

3. Axial magnetic field strength for SERT II and scaled 20-cm thrusters compared 2

4. Iron filing arrangement produced by the magnetic field of a 10-magnet thruster, cathode removed 3

5. Iron filing arrangement produced by the magnetic field of a 10-magnet thruster, cathode in place 4

6. Discharge chamber losses as a function of propellant utilization efficiency for 6- and 8-magnet thrusters 5

7. Discharge chamber losses as a function of propellant utilization efficiency for a 20-cm-diam 10-magnet scaled thruster 5

8. Discharge chamber losses for SERT II and scaled 20-cm-diam thrusters compared 7

Abstract

A 20-cm-diam electron-bombardment ion thruster was constructed by scaling a smaller high-performance flight-type unit. The scaling was not exact inasmuch as differences existed in the mercury propellant distribution, anode geometry, cathode type, and cathode location. An additional magnetic field also existed due to the spiral configuration of the cathode used. The performance of the scaled unit is presented. Ion chamber losses equivalent to those presented for the flight-type thruster were obtained.

Scaling of a High-Performance Ion Thruster

I. Introduction

Recent studies (Refs. 1, 2) have indicated that ion thrusters operating at a power level of 2.5 kW are of interest for solar powered missions. Experimental work on an array of four 20-cm-diam electron-bombardment mercury ion thrusters designed to operate at this power level is under way at the Jet Propulsion Laboratory. Initial results are described in Ref. 3 and an improved electromagnetic thruster is described in Ref. 4. Present ion chamber performance, however, is still somewhat less than that presented for the flight-type permanent magnet, the SERT II thruster described in Ref. 5. The high-performance 15-cm-diam flight-type thruster was therefore scaled to examine the effects on ion chamber performance of magnetic field shaping of the 20-cm-diam thruster and also to provide a permanent-magnet thruster. For a given mission this thruster might be useful if the external magnetic field could be minimized or acceptable as far as the science experiments are concerned.

II. Thruster Scaling

A diagram of both the high-performance thruster (SERT II) and the 20-cm-diam scaled unit is shown in Fig. 1. Scaling of the 15-cm-diam thruster to the larger

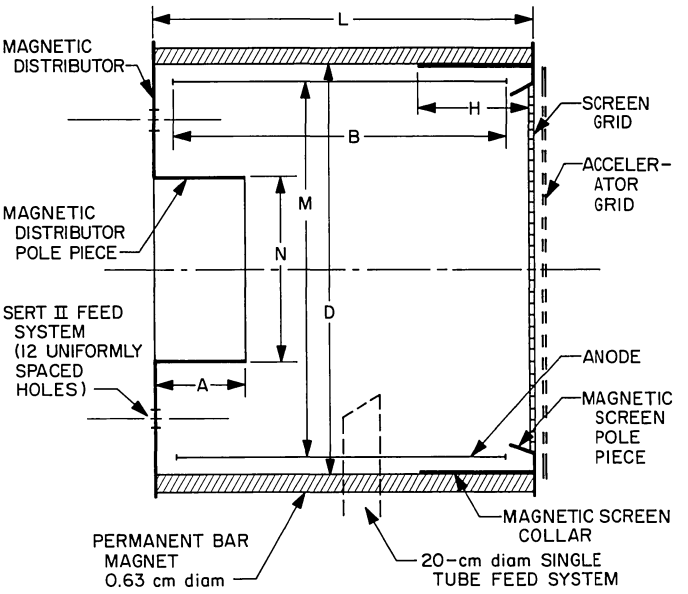

DIMENSIONS IN CENTIMETERS

THRUSTER	A	B	D	H	L	M	N
SERT II	3.18	11.4	17.5	3.8	12.9	15.0	6.3
20-cm	3.8	10.2	21.7	3.8	15.9	20.0	7.6

Fig. 1. SERT II and scaled 20-cm-diam thrusters compared, cross-sectional sketch

diameter was accomplished by simple geometric scaling of the lengths and diameters of the soft steel components and the overall thruster length. The soft steel parts were all constructed of 0.081-cm-thick material (1020 steel).

A photograph of the scaled thruster is shown in Fig. 2. The majority of thruster data presented here was obtained using a spiral-wound nickel-mesh cathode of the type described in Ref. 6. A tantalum ribbon cathode was also used during the study to evaluate the effects of the spiral configuration. Both cathode types were nominally located at the downstream end of the magnetic distributor pole piece.

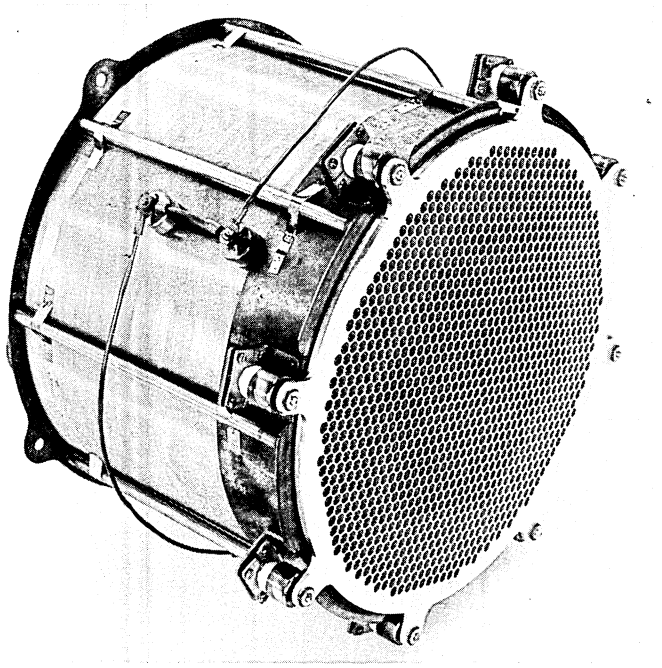

Fig. 2. The 20-cm-diam permanent magnet electron-bombardment ion thruster

The thruster tests employed six, eight, and ten 0.635-cm-diam Alnico V rod magnets. Six equally spaced magnets on the thruster diameter produced a field in which the product of the anode diameter and the magnetic field was approximately equal to that of the smaller thruster, a quantity indicated desirable in a previous scaling study (Ref. 7). Eight and ten magnets produced proportionately higher fields. The resulting field configurations, plotted in Fig. 3, are compared with the SERT II thruster. The field shape was a fairly close

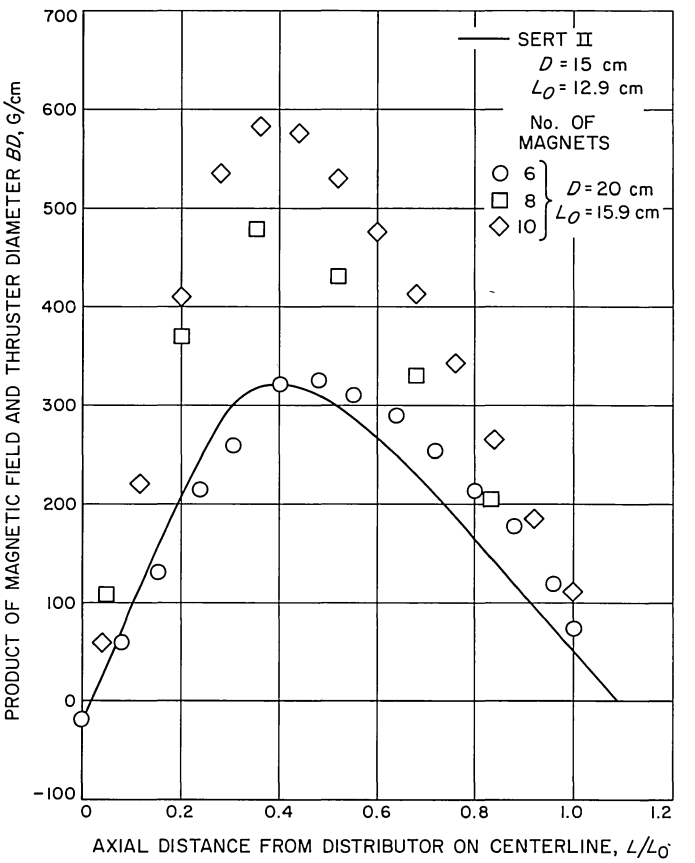

Fig. 3. Axial magnetic field strength for SERT II and scaled 20-cm thrusters compared

approximation of that obtained from the smaller thruster with the cathode removed. Magnetic parts within the cathode increased the field by approximately 10% near the cathode location. Figure 4 is a photograph of the iron filings arrangement produced by the magnetic field with the cathode removed. Figure 5 shows the iron filings with the cathode in place.

The accelerator system consisted of two molybdenum grids. The grid holes in both the screen and accelerator were 0.476 cm in diameter. The thicknesses of the screen grids were 0.127 and 0.254 cm. The grid separation was 0.178 cm. The total grid opening area was 245 cm^2 (78% of the total area within the diameter of the anode).

Propellant entered the thruster approximately 6.35 cm from the screen grid. The feed line was attached to the housing and passed through the anode. Propellant was distributed from a slot and was directed generally toward the cathode. Mercury flow was fed and measured from an external burette.

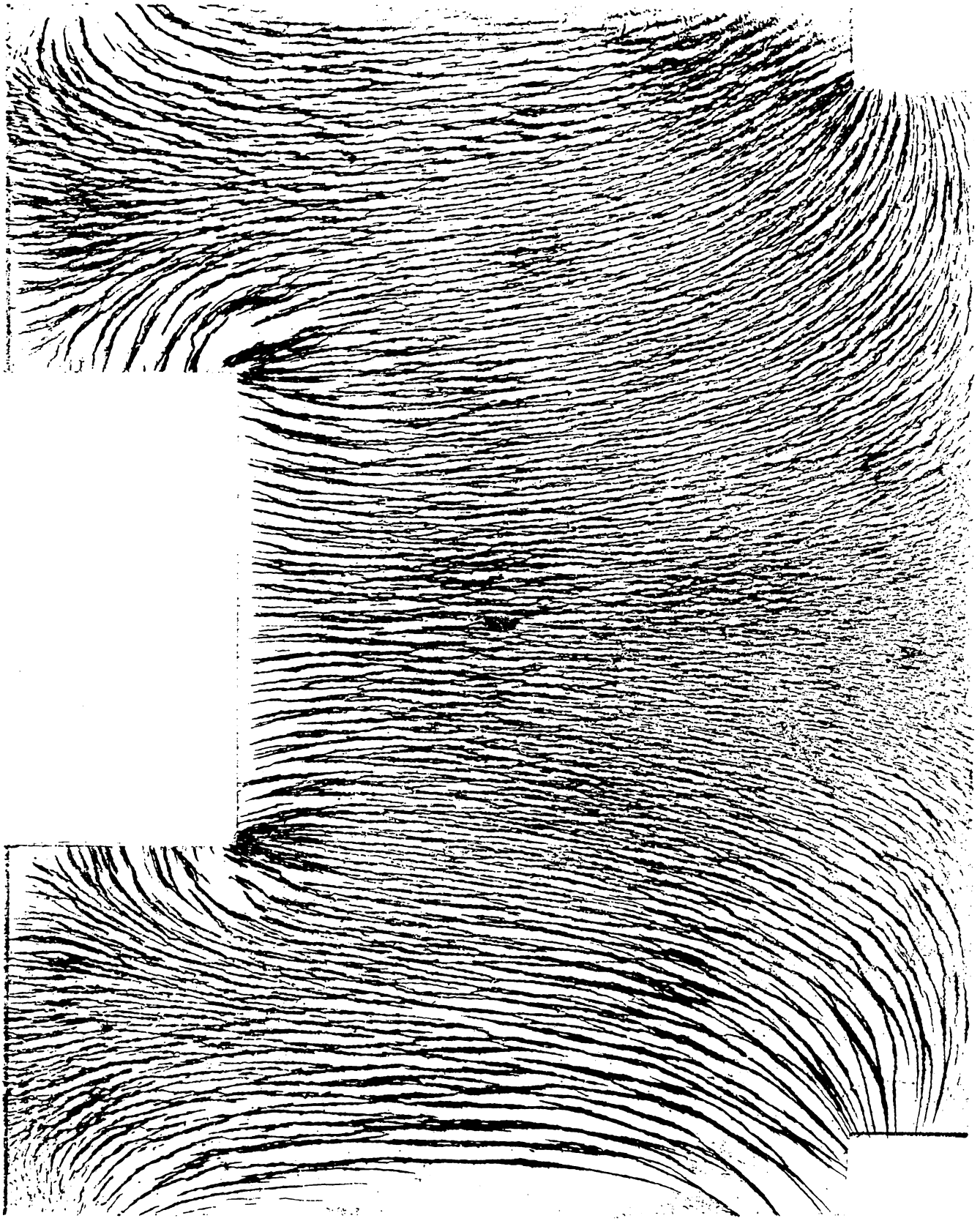

Fig. 4. Iron filing arrangement produced by the magnetic field of a 10-magnet thruster, cathode removed

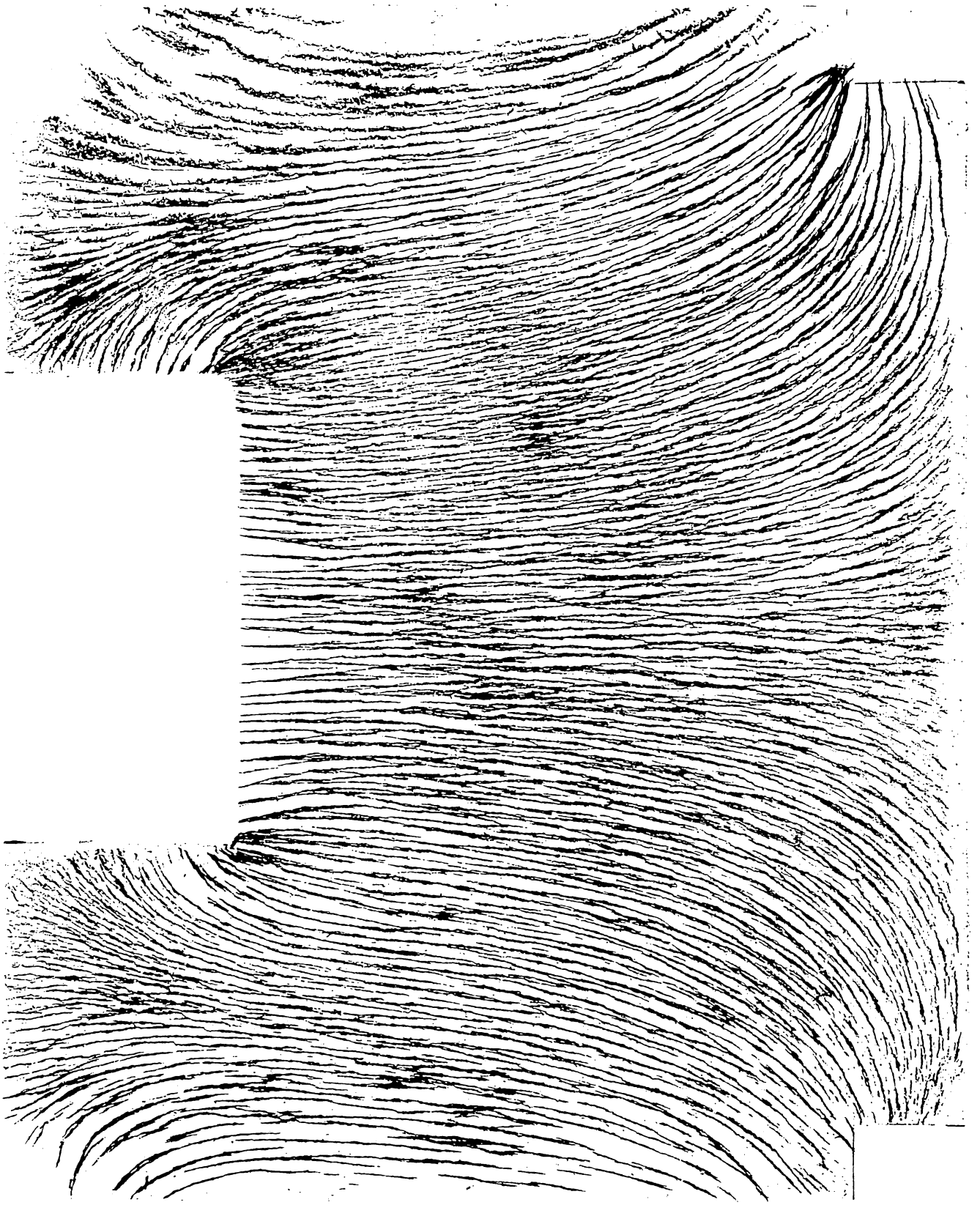

Fig. 5. Iron filing arrangement produced by the magnetic field of a 10-magnet thruster, cathode in place

III. Thruster Operation

The performance of the scaled 20-cm-diam thruster is presented (Fig. 6) for both 6- and 8-magnet configurations. Discharge chamber losses (discharge chamber power/ion beam current) are plotted against propellant utilization (ion beam current/mercury flow in equivalent amperes of singly ionized mercury). The scaling was not exact and some differences existed between the two thrusters. The primary differences are listed as follows:

(1) Cathode type, material, and location.

(2) Method of propellant introduction and distribution.

(3) Anode geometry.

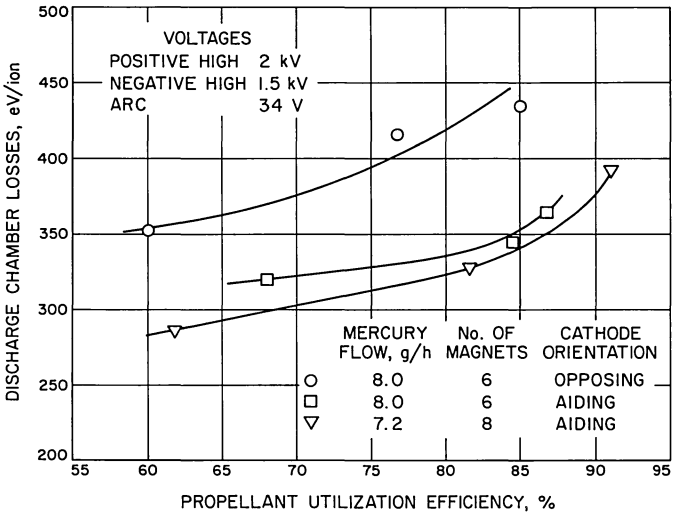

Fig. 6. Discharge chamber losses as a function of propellant utilization efficiency for 6- and 8-magnet thrusters

The cathode used had a spiral heating element that generated a magnetic field on the order of 3 G for the levels of dc cathode heating current used. This field was significant when compared with the field generated by the permanent magnets and by its orientation could affect thruster operation. Data for the 6-magnet thruster with the cathode field aiding and opposing the thruster field is included in Fig. 6. The aiding field was observed to result in lowest discharge chamber losses and this field was therefore used on thrusters that employed a larger number of magnets.

Thruster operation with 8 magnets demonstrated some improvement over that with 6 magnets. In addition, the 8-magnet configuration was operated with a refractory ribbon cathode to evaluate the effect of the field generated by the cathode. The ion chamber losses were generally higher with the refractory cathode and increased rapidly with increasing propellant flows, while the thruster was maintained at a constant propellant utilization. It appears that additional field in the vicinity of the

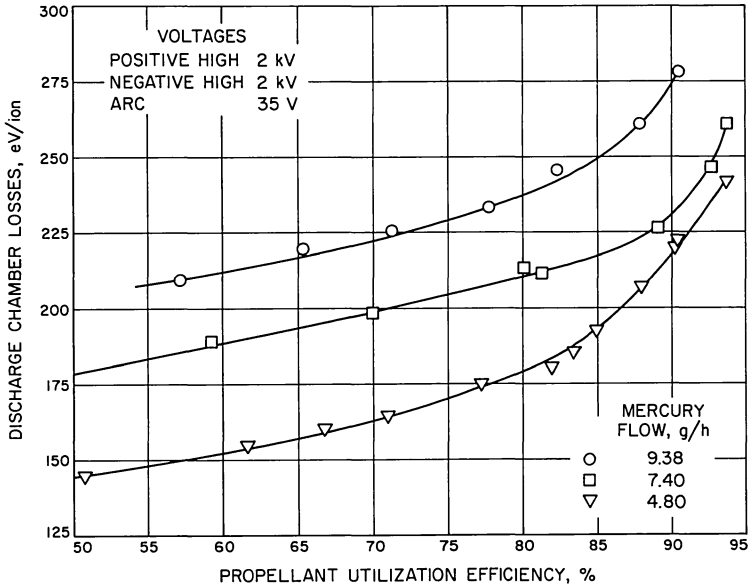

Fig. 7. Discharge chamber losses as a function of propellant utilization efficiency for a 20-cm-diam, 10-magnet scaled thruster

cathode can provide lower ion chamber losses. It might also provide a possible solution to the thruster instabilities at low discharge voltages observed in Ref. 5.

Thruster operation with 10 magnets also utilized a thin (0.127-cm) screen grid, which had been found desirable (Ref. 4). Thruster operation for a range of three flow rates is presented in Fig. 7. The screen thickness plus grid separation for this run was 0.305 cm, which corresponded fairly closely with the 0.330 cm used for the smaller thruster. Further reductions in both screen thickness and grid separation are possible and could produce some additional improvements in ion chamber performance. Typical thruster operation for the 10-magnet configuration at four operating points is presented in Table 1.

A comparison of the scaled thruster operation with that of the high performance thruster (Ref. 5) was made at equivalent voltages and flow rates. The ion chamber losses, shown in Fig. 8, were found to be in close agreement for the thrusters of both sizes. The 20-cm-diam

Table 1. Typical thruster performance data for a 10-magnet configuration

Operating parameters	Operating points			
	(1)	(2)	(3)	(4)
Positive high voltage, kV	2	2	2	3
Negative high voltage, kV	2	2	2	2
Negative high voltage current, A	0.00950	0.00610	0.00290	0.00205
Beam current, A	1.030	0.800	0.495	0.440
Arc voltage, V	35	35	35	30
Arc current, A	7.25	4.85	2.48	2.90
Cathode voltage, V	5.0	4.5	4.2	5.3
Cathode current, A	37.0	35.5	34.0	41.0
Vaporizer voltage, V	1.1	1.0	0.85	0.9
Vaporizer current, A	2.9	2.6	2.2	2.4
Manifold heater voltage, V	5.0	5.0	5.0	5.0
Manifold heater current, A	1.0	1.0	1.0	1.0
Mercury flow rate, g/h	9.38	7.40	4.80	4.00
Computed parameters				
Beam power, kW	2.060	1.600	0.990	1.320
Drain power, kW	0.038	0.024	0.012	0.010
Cathode power, kW	0.185	0.160	0.176	0.217
Arc power, kW	0.253	0.170	0.086	0.087
Vaporizer power, kW	0.003	0.003	0.002	0.002
Manifold power, kW	0.005	0.005	0.005	0.005
Total thruster power, kW	2.544	1.962	1.271	1.641
Thrust, 10^{-3} lb	21.3	16.6	10.2	11.2
Power-to-thrust ratio, kW/lb	117.5	118.1	124.6	146.5
Power efficiency, %	81.0	81.6	77.9	80.4
Electrical specific impulse, s	4460	4460	4460	5460
Source energy per ion, eV/ion	246	212	175	198
Propellant utilization efficiency, %	82.2	81.0	77.3	83.2
Effective specific impulse, s	3670	3610	3450	4540
Total thruster efficiency, %	66.6	65.1	60.2	66.9

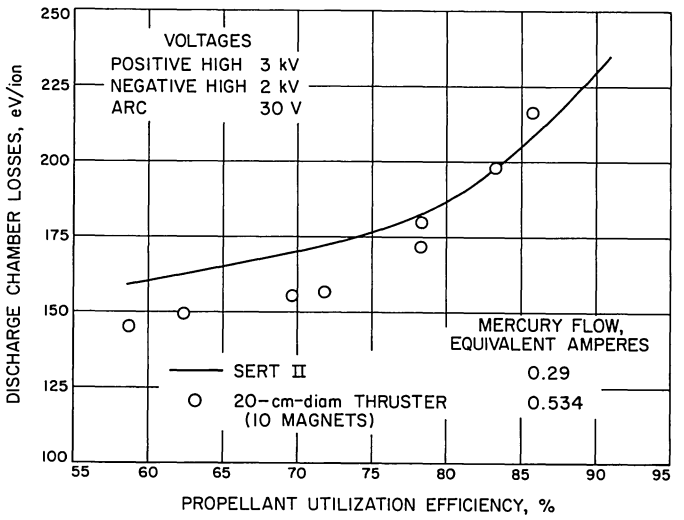

Fig. 8. Discharge chamber losses for SERT II and scaled 20-cm-diam thrusters compared

thruster operated at 205 eV/ion at 85% propellant utilization. The maximum utilization was about 86%, which was less than that obtained for the smaller thruster, but was found to increase as the arc voltage was increased. The discharge chamber stability was found to be a function of the propellant flow and was stable down to about 25 V for low flow operation (4 g/h).

IV. Conclusions

The ion chamber losses in a 20-cm-diam ion thruster, with a magnetic field scaled from a smaller high-performance thruster, were found to be equivalent to those obtained with the smaller thruster when operating at an equivalent plasma density. Higher magnetic fields were found compatible with stable thruster operation of the larger unit with no limiting instabilities noted for the range of magnetic fields and discharge voltages investigated.

An additional magnetic field due to the cathode configuration existed near the cathode location, preventing an exact field scaling. The effects of an additional magnetic field in this vicinity have not been fully evaluated, but appear to improve thruster performance. No attempts were made to reoptimize the larger thruster at the higher magnetic field strengths.

References

1. Kerrisk, D. J., and Kaufman, H. R., "Electric Propulsion Systems for Primary Spacecraft Propulsion," AIAA Paper No. 67-424, July 1967.
2. "Solar Powered Electric Propulsion Spacecraft Study," Report No. SSD-50094R (Final Report on JPL Contract No. 951144), Hughes Aircraft Company, Culver City, Calif., Dec. 1965.
3. Masek, T. D., and Womack, J. R., "Experimental Studies with a Clustered Ion Engine System," AIAA Paper No. 67-698, Sept. 1967.
4. Masek, T. D., "Clustered Ion Engine Systems Studies," in *Supporting Research and Advanced Development,* Space Programs Summary 37-48, Vol. III, pp. 131–134. Jet Propulsion Laboratory, Pasadena, California, Dec. 31, 1967.
5. Bechtel, R. T., "Discharge Chamber Optimization of the SERT II Thruster," AIAA Paper No. 67-668, Sept. 1967.
6. "Development and Test of an Ion Engine System Employing Modular Power Conditioning," Report No. SSD-60374R (Final Report on JPL Contract No. 951144), Hughes Aircraft Company, Culver City, Calif., Sept. 1966.
7. Reader, P. D., "Scale Effects on Ion Rocket Performance," *ARS J.*, Vol. 32, No. 5, pp. 711–714, May 1962.